Comparative analysis of *Xenopus* mesonephric transcriptomics: Conservation of the developmental lineage of nephron stages

Mark E. Corkins [1,2], Adrian Romero-Mora[1], MaryAnne A. Achieng[3], Nils O. Lindström[3], and Rachel K. Miller[1,5-7]

[1] Department of Pediatrics, Pediatric Research Center, UTHealth McGovern Medical School, Houston, Texas 77030
[2] Department of Cell, Developmental & Regenerative Biology, Icahn School of Medicine at Mount Sinai, New York, NY. 10029
[3] Department of Stem Cell Biology & Regenerative Medicine, Keck School of Medicine of USC, Los Angeles CA. 90033
[5] Department of Genetics, University of Texas MD Anderson Cancer Center, Houston, Texas 77030
[6] MD Anderson Cancer Center UTHealth Graduate School of Biomedical Sciences, Program in Genetics and Epigenetics, Houston, Texas 77030
[7] MD Anderson Cancer Center UTHealth Graduate School of Biomedical Sciences, Program in Biochemistry and Cell Biology, Houston, Texas 77030

*Corresponding Author: Mark.Corkins@mssm.edu ; Tel.: +01-212-241-1757

Keywords: mesonephros; kidney; nephron; *Xenopus*; scSeq; single-cell mRNA sequencing, mesonephros

Abstract

The mammalian kidney develops in three sequential stages referred to as the pronephros, mesonephros, and metanephros, each developing from the preceding form. All three phases of kidney development utilize epithelized tubules called nephrons, which function to take in filtrate from the blood or coelom and selectively reabsorb solutes the organism needs, leaving waste products to be excreted as urine. The pronephros are heavily studied in aquatic organisms such as zebrafish and Xenopus, as they develop quickly and are functional. The metanephros is a preferred mammalian kidney model, as it best recapitulates human disease. However, very little is known about the mesonephric stage of kidney development in any organism. The pronephros extend to form the mesonephric duct, which ultimately develops into the Wolffian duct in male amniotes. Meanwhile, in organisms that lay their eggs in aquatic environments, the mesonephric kidney is the final form that is generated. Therefore, further understanding of the development and physiology of these kidneys will provide insight into the urogenital system as well as its evolutionary conservation. To gain a better understanding of its structure and cell types, we analyzed the developing mesonephros by in situ and single-cell mRNA sequencing of cells the that make up the developing mesonephros. By comparing these data to those published for the *Xenopus* pronephros and mammalian metanephros, we were able to evaluate nephron conservation between the three kidney stages.

Introduction

The kidney is a structure that functions to secrete soluble waste products from an organism. It performs this function through epithelial tubes called nephrons. The specialized tubules that make up each nephron take in fluid from the coelomic cavity or vasculature, reabsorb solutes that the organism requires, such as proteins, carbohydrates and salts, leaving waste products to be excreted as urine. In freshwater organisms, nephrons remove the excess water, whereas in terrestrial animals, nephrons resorb water and therefore concentrate waste. Because the function of each nephron depends on the patterning of solute carriers and ion channels, they express different genes within specific regions along the proximo-distal axis.[1-3] Several kidney diseases preferentially manifest within specific nephron segments, such as some cystic kidney disease and glomerulopathies indicating the differences in development and function of these distinct nephron segments.[4-7]

The mammalian kidney develops in three consecutive forms with each exhibiting a more complex arrangement of nephrons. The three stages are referred to at the pronephros, mesonephros and the metanephros.[8, 9] The first kidney form is the pronephros,[10] which consists of a single nephron that originates in the cervical region of the intermediate mesoderm.[11] In fish and amphibians, this structure is functional and performs many of the functions of the nephrons in subsequent versions of the kidney.[12, 13] The most posterior region of the pronephros gives rise to the nephric duct, which is retained throughout development and provides the structural foundation of the later forms. The second form of the kidney is the mesonephric kidney, which forms in the caudal intermediate mesoderm. This structure is made up of multiple nephrons that converge onto the nephric duct.[14] This form contains true glomeruli connected to the vasculature.[15] In fish and amphibians this is the final adult kidney form, whereas in mammals it is restructured into the Wolffian duct of the male reproductive tract.[16] In amniotes, a third kidney stage develops called the metanephros. This structure forms in the sacral region of the intermediate mesoderm and is started by a process of branching of the pronephric duct.[17, 18] Although each of these kidney forms are known to carry out similar function, and are formed by a process of epithelization from the mesenchyme, the conservation in the cell types between kidney stages yet to be evaluated.

The development of the mesonephric kidney is poorly studied in any organism.[14, 19] In *Xenopus* and zebrafish, the pronephros is the preferred version of the kidney to use for kidney studies as it develops quickly, is functional, able to be directly visualized through the epidermis. This form has also been used to model many diseases seen in the mammalian metanephric kidney.[20-22] In mammals, the metanephric kidney is the preferred

structure to study as it best models diseases seen in human, and can be studied after the birth of the organism.[23, 24] This means the mesonephric kidney largely gets overlooked. Much of what we know about the mesonephros is derived from structural observations of the fully formed mesonephric kidney in aquatic organisms or indirect observations when looking at the earliest processes involved in metanephric development in mammals.[15, 25-28] The majority of what we know about gene expression in the mesonephros comes from a small set of genes studied in zebrafish and mouse.[29, 30]

It is hypothesized that each successive form of the kidney reuses the same genetic programming to recreate a nephron with a similar cellular makeup. This is supported by multiple studies that shows that many of the phenotypes seen in the mouse or human metanephric nephrons are recapitulated in the frog and zebrafish pronephros.[31] Additionally, single-cell sequencing (scRNA-seq) and in situ analysis of the functional *Xenopus* pronephros shows a conserved genetic profile to the adult mouse metanephric kidney.[12, 32, 33] However, as this comparison was between two different species the degree of conservation is hard to measure. Currently studies to directly compare the cell types observed in the different forms of the kidney have yet to be performed.

The goal of this study is to utilize comparative analysis to gain a better understanding of the cell types within the mesonephric kidney in *Xenopus laevis*. To accomplish this, we used transgenics, immunostaining, *in situ* analysis and scRNA sequencing to understand the cell types within the developing and mature mesonephric kidney. We find that early and late cell types are conserved but develop differently and end up with a conserved genetic profile.

Materials And Methods

For detailed methods see supplemental material.

P*pax8*::GFP$^{<\ NXR_0132>}$ cryo-sperm was used via standard protocols. [34, 35] Insitu and antibody staining was performed using previously established protocols. [36, 37] scRNA-seq was performed at UTHealth Cancer Genomics Center (CGC) and processed using Seurat. [38, 39]

Results

<u>*Evaluating the timing of mesonephric development*</u>

As a starting point to visualize early development of the mesonephros, we used P*pax8*::GFP transgenic animals (Fig 1A). For staging, we used the development of the limb buds as an indicator of the developmental stage. However, for the same stage, as indicated by the limb bud, the kidney development can, even in the same batch of embryos. In *Xenopus*, the Ppax8::GFP and pax8 in situ probes are well-characterized pronephric nephron markers.[40] *pax8* is expressed in both kidney epithelium as well as the nephron progenitor cells in both the *Xenopus* pronephros as well as the mammalian metanephros.[41-43] The first signs of nephron formation for the mesonephros are observed around stage 46. Surprisingly, the first nephrons began forming near the posterior end of the nephric duct rather than the anterior end as anticipated. The formation of new nephrons becomes difficult to recognize after stage 53 when the large number of nephrons and the formation of melanocytes hinder the visualization of new nephrons. As anticipated, these nephrons are composed of a typical ciliated cuboidal epithelium (Fig1 B).

To determine when the mesonephric kidney becomes functional, we modified a technique describe by Zhao and Vize 2004 that injects labeled molecules into the vasculature or coelomic cavity then directly visualizes their flow through the kidney.[12, 44, 45] As the mesonephric kidney can't be directly visualized in living animals more stable dyes were chosen. We used a mixture of Hoechst 3342 and EC-Lectin (Erythrina Cristagalli) into the heart of *X. laevis* (Fig 1 C,D). The Hoechst stains the nuclei of most cells within the tissues it circulates through, including the vasculature and coelomic cavity to show the dye was injected. EC-Lectin is a non-cell permeable stain that labels the lumen of the proximal tubules of the pronephric nephron in early tadpoles, and those of the mesonephros in later tadpoles. Therefore EC-lectin should only stain tubules if it flows through the nephron. The level of lectin staining is highly variable from embryo to embryo, and many injections do not visually stain the either the pronephros or the mesonephros. The pronephros was used as a positive control, as we did not detect any mesonephric staining without pronephric staining as well. The mesonephric kidney begins to stain around stage 50, suggesting the first nephrons are functional around this point.

Transcriptome analysis of the mesonephros

To obtain a cellular makeup of the mesonephric kidney, single-cell mRNA sequencing analysis was performed. Stage 50-52 kidneys were chosen, during which time nephrons become functional, yet it is still possible to obtain mesonephric progenitor cells, given that the kidney is still growing. Additionally stage 52-56 kidneys were chosen as the kidney is thin enough to be stained in wholemount, and many samples could be obtained

in a relatively short period of time (~3 weeks). Also, the kidney is functional at this point (Fig 1 C, D). At this stage the kidney is easily identifiable without markers, as the connective tissue enveloping the ventral side of the kidney is covered in pigment cells (Fig 2A). 100 mesonephric kidneys were manually dissected from heavily anesthetized animals. The kidney is being held under tension and upon dissection the kidneys shrink along their anterior posterior axis upon dissection. We obtained approximately $1x10^7$ cells in total. After sequencing a large number of cells were removed due to low reads count, therefore we erred toward potential removal of good cells with low read count to prevent the inclusion of poorly sequenced cells or cell fragments from altering the results. After removing all bad cells, 14,411 cells were left with an average read depth of 34,500 reads per cell.

As the nomenclature for the *Xenopus* nephron has changed many times, for this study, when possible, we will use the segments described in (Corkins et al. 2023) for the pronephric nephron. Clustering and UMAP analysis was performed independently of the previously published scRNA-seq for the pronephros to prevent bias in our clustering and analysis.[33] To prevent non-kidney cells from altering our analysis we separated them away from the kidney cells. Canonical genes for the Xenopus pronephros and mouse metanephros were used to identify the cells makeup of the mesonephros. Mesonephric cells were identified by expression of *cdh1*, *cdh16*, *hnf1b*, *atp1a1*, *nphs2*, and *foxi1* and subclustered away from non-kidney cells such as red blood cells (Fig 2B, C, S1). Any clusters that associated with these sets via UMAP (Uniform Manifold Approximation and Projection) were included in the kidney subset. The cell types that were not used for this analysis include 3 types of white blood cells 2 types of endothelia, and red blood cells, all other cells showed some association with the kidney subpopulation (Fig S2).

We identified many the same cell types as was identified in the pronephric single cell dataset which were numbered 1-6 to match the pronephric scRNA-seq set. These cell types break down into three broad categories proximal distal and duct cells. The duct cell includes both principal and intercalated cell types. Expected cell types unique to the mesonephros were also identified including an immature parietal epithelial cell type, and three stromal cell types. The stromal cell types break down into two ECM producing fibroblast type and one smooth muscle type. All the nephron cell types were connected by intermediate cell types which include a central group of cells that express markers of nephron progenitor cells such as *six1* and *six1* were

identified.[46, 47] These more progenitor-like cell types were labeled with an “e” for embryonic (eg. 2e, 3e, 5e). (Fig 2D).

Comparative transcriptomics of Xenopus nephron forms

To determine the similarities and differences between the *Xenopus* kidney stages, the pronephros and mesonephric datasets were integrated (Fig 3). To do this the pronephric data was reprocessed using the new X. laevis 10.1 genome. Outside of the cell types previous described the most distinct difference was that the distal cluster x6a from the pronephros did not co-cluster with the equivalent cells of the mesonephros. These are the cells of the most distal duct. In the pronephros these cells are likely either cloaca or epidermal cells, whereas in the mesonephros they are most likely developed from the most distal principal cells of the pronephros which could account for these diferences.

In the mesonephros, more intercalated cells were sequenced, allowing for a more detailed analysis of this cell type. These cells segregated to the two groups which correlate with the two types of intercalated cells found in the mammalian kidneys called type A and type B, which are denoted as x6b1 and x6b2 respectively. Also, a small group of cells express extracellular proteases *(mpo*, *mmp7*, *mmp9*, *prtn3*, *prss57*). These markers indicate that these cells are likely a mobile cell type and therefore labeled as Mobile. Outside of these proteases these cells also have markers of cluster x2a the most proximal tubule cell of the kidney. Suggesting that the proximal tubules are migrating within the kidney as the nephron grows.

Within each of the nephron segments surprisingly few differences were identified between the pronephros and the mature mesonephric segments. *irf1*, *btg2*, *fosl1* and *jun* were identified to be more highly expressed in the pronephros. This is likely due to the differences in nephron maturity, and stress induced from the disassociation process. The other differences were the expression of the hemoglobin genes *hbe1* and *hbd.* Though it is unclear why these genes are more expressed in the pronephric tubules. The only surprising gene difference we identified is in the *lhx1* gene. In the pronephros lhx1 is a key gene required for the formation of the nephron and is expressed ubiquitously in the nephron prior to epithelization. Following epithelization, it is limited to the nephrostome and migrating duct cells after epithelization.[48, 49] However, in the mesonephros lhx1 expression is retained in the principal cluster 4. In mouse a similar expression is seen where it is expressed

early then its expression becomes limited to the distal convoluted tubules. With the exception of *lhx1* this data suggests that the expression profile for each cell types is highly conserved, across kidney stages.

Mesonephric progenitor lineage

Given the presence of both mature nephrons as well as those at early developmental timepoints within the mesonephros, analysis as to how these nephrons segments develop was carried out (Fig. 3 A-C). Less differentiated cells were identified by early kidney markers *wt1*, *six1, meis1*, and *lhx1.* These cells were labeled with the “e” designation (Fig 2C). To find the more differentiated cells we looked for transcriptional characteristics of these cells. Firstly, the more differentiated cells express of more mature markers such as transporters and junctional components (Fig 2E). Additionally, they co-cluster with the mature pronephric cells (Fig 3A). Thirdly, as more differentiated cells tend to suppress cell division and stall in G1/G0 phase. To identify cells that are undergoing cell division, published gene sets of S-phase, and G2/M phase markers and that are commonly used to identify dividing cells in mouse and human were used.[50] Cells were labeled by phase due to enrichment of these genes (Fig 4A). We find that these cells are also more G1 enriched.

To identify possible developmental pathways, we utilized the Monocle 3 library for R (Fig 4B-D).[51] Early intermediate and late gene expression was verified for markers of each lineage (Fig 4 F-H). The paths varied slightly pending how the UMAP and clustering was performed in Seurat, however certain features were constant. There appears to be four branches that occur from the embryonic cells. 1.) The stromal and multiciliated cells. 2.) the podocytes and parietal cells 3.) the proximal tubules, and 4.) the distal nephron segments (intercalated, principal, and distal cells). The separation between the podocytes, stromal, and multiciliated cells was more easily observed when subclustered away from the more developed cells (Fig 4E). These four branches are similar to what is observed in the mammalian mesonephric kidney and show similar genetic markers of these branches (Fig 4G-I). This analysis indicates that nephron progenitor cells produce three primary nephrogenic lineages, which are the foundation of the proximal, distal/principal/ionocyte and stomal/glomerular developmental trajectories.

Evolutionary conservation of kidney development

To determine whether the developmental lineage of the nephron is conserved, comparisons between the *Xenopus* mesonephros to the mammalian metanephric kidneys were performed. The *Xenopus* mesonephric

scRNA dataset was integrated with the Mouse adult (Fig 5), by a method similar to what was done for the pronephros. The mouse metanephros is fully formed and, therefore, has fewer undifferentiated cells relative to the *Xenopus* mesonephros. Given the similarity between the pronephros and mesonephros it was unsurprising that we found a strong level of conservation between the mature cells of the Xenopus mesonephros and mouse adult metanephric kidney. As we found the pronephros cells that don't have a clear analog tend to associate with Loop of Henle. Therefore, the multiciliated cells, and nephron progenitor cells group around the LOH cells.

Spatial positioning of cell types within the mesonephros

In order to determine the anatomical positions of the cell types identified in the *Xenopus* mesonephros, the spatial expression patterns of known kidney markers were analyzed.

We set out to identify the location of the kidney progenitor cells. In the pronephros *pax8* and *lhx1* are commonly used to label early pronephric cells, although *pax8* labels the nephron progenitor cells of the pronephros and mammalian metanephros, P*pax8*::GFP transgene expression was only observed in epithelized tubules of the mesonephros (Fig 1A). Unlike pax8 which is constitutively expressed in the entire nephron *lhx1* is only present in the pronephric kidney mesenchyme, with its expression decreasing shortly after epithelization. However, neither Lhx1 protein nor *lhx1* mRNA was detected using antibody staining or in situ analysis before stage 50.[48, 49] However, expression in the brain, and a weak signal was visible in the nephrons around the midline of the two kidneys in stage in later stage 52 embryos (Fig S1B). This signal is indistinguishable from the *lhx1* identified in the early principal cells of cluster 4. Therefore as an alternative target *six1* was identified by scRNA sequencing to be specific for nephron progenitor cells in the mesonephros, and had been used in in the mouse as a transient early marker of the kidney progenitor cells.[52] A *six1* probe was cloned from cDNA and *in situ* analysis was done. Staining was observed in strongly some collagenous structures of the head, and there a weak signal was noted in the somatic myotome. Early in mesonephric development, *six1* is found stripes of cells behind the nephric tubules (Fig S1C). At around stage 50, *six1* is found scattered around the kidney with enrichment around the dorsal midline (Fig 6A), and in the more developed kidney (Stage 53) a string of *six1* positive clusters is found on the dorsal side of the kidney. This suggests that new nephron formation adjacent to dorsal midline structures. Given the weak signal, the limited

number of early progenitor cells identified in the scRNA-seq we predict that these cells are rare and only exist for a short period of time.

We wished to obtain a better special layout of the mesonephric kidney. As an first approach FITC labeled Erythrina Cristagalli (EC)-Lectin were used to label the proximal tubules (Fig 6B).[53] The proximal tubules were largely labeled at the more lateral sides of the kidney and labeled the largest percentage of the kidney, suggesting that most of the nephron is composed of proximal tubules. *In situ* probes for *slc5a1* was also confirmed this expression pattern (Fig 6C).[32, 54, 55]

Outside of the proximal tubules the location of other structures was visualized by *in situ* analysis. All the probes used were published to work in the early *Xenopus* and show expression by scRNA-seq. *nphs1* was used to stain the podocytes, which are part of glomerulus/glomus.[56] These podocytes label puncta along the medial sections of the kidney and mark the most proximal segment of the nephron. The positioning of the renal artery is positioned down the midline of the two kidneys coincides with the inflow into the kidney is oriented toward the midline. This patterning has been described in other studies using EM to look at the vasculature of the mesonephros in *Xenopus.*[15] *irx1* and *irx3* were used to label the distal tubes.[57] Individual tubules were found along the medial edge of kidneys. *Mecom* (*evi1*) and *clcnkb* were used to stain the distal and principal cells.[58-60] These genes more strongly label tubules along the midline, however weak projections towards the collecting duct were visible along the dorsal side of the kidney. Though labeling of the principal cells were stronger the expression pattern was similar to that seen for the *irx1/3* genes. *foxi1* was used to label the ionocytes/intercalated cells of the duct.[61] *foxi1* labels a set of converging tubules along the dorsal side of the kidney.

This provides an image where much of the initiation of nephrogenesis likely occurs medially as this is where six1 is expressed. The proximal tubes expand laterally making up the greatest proportion of the kidney (Fig 6D). The proximal tubules flown into the distal tubules which are positioned near the glomeruli medially located. The distal tubule then flows into the mesonephric duct which then merges with other mesonephric ducts ultimately being excreted from the kidney via the pronephric duct.

Discussion

As little is known about the mesonephric kidney, this study provides novel insight into its structure, function and development of the mesonephric kidney. *X. laevis* was chosen largely because the pronephros single-cell sequencing was performed using *X. laevis* allowing for a direct comparison between two kidney forms.[33] *X. tropicalis* and zebrafish were possible alternatives. However, they have a smaller mesonephric kidney, and thus would require more kidneys to be dissected and more time required to get to perform single-cell transcriptomic analysis. This study utilized staining techniques and single-cell sequencing to gain a better understanding the structure and cell types within both developing and mature mesonephric nephrons.

At stage 53, approximately 20-30 glomeruli were observed, many fewer than are present in the adult kidney, and much less than the estimated 2000 nephrons that is fomed.[15, 62] Additionally, the more posterior nephrons were the first to develop, suggesting sequential formation of the nephron from posterior to anterior. This suggests that nephrons likely develop asynchronously over a long period of time, a phenomenon seen in the mammalian metanephric kidney. In humans the first glomeruli will form around week 9 and the approximately 250 thousand to 1million nephrons will form over the next 27 weeks.[63]

Unlike what was observed in the pronephric analysis, very few non-nephron cells were identified.[33] This is likely due, in part, to the membrane that surrounds the mesonephric kidney isolating it from nearby tissues. Therefore, other cells do not contaminate the dissected tissue. Associated cells were obtained, including endothelial cells and blood cells (Fig S1). These cell types were expected these to be present, given that they are associated with the kidneys as they become functional.

Reports suggest that the first signs of germline formation occurs around stage 52, [64, 65] and though the mesonephric kidney contributes to male reproductive organs, and we performed scRNA-sec around this timepoint we were unable to distinguish sex. Similar to the pronephros, looking at the common markers of sex such as *dmrt1, foxl2, dm-w* or using the genes that were sexually dimorphic in mouse did not reveal any patterns of sexual dimorphism in the kidney. These genes were either completely absent or ubiquitous in the proximal tubules. However, most of these studies were carried out before the genetic determinants of sexual differentiation were determined in *Xenopus.*[66]

Cluster 4 (early principal cells) is an unusual cell type and may be unique to amphibians. The expression profile, and comparison with the mouse indicates that it is similar to that of principal cells. However,

pseudotime analysis suggests that it develops from the distal tubules instead of directly form the kidney progenitors. Even more puzzling, the two most highly expressed transporters found in this type are *slc4a4* and *slc9a3,* which encode proteins necessary for pH balance within the proximal tubes of mammals.[67] In the *Xenopus* pronephros, cluster 5, that is more distal to cluster 4, however cluster 4 associated better with the cells of the more distal collecting duct in mice, putting it out of order. The physical position of this cluster is unclear from in situ analysis, slc4a4 expression is not near the other distal or principal cells as expected. This indicates a unique cell type that integrates the gene expression profile of multiple different cell types.

A strong similarity exists between the transcriptional profile of the more mature cells of the *Xenopus* mesonephros and pronephros. Given these similarities, it is likely that these nephrons reuse the same developmental programming for generation of nephrons in each stage. However, as we don't currently have good data for the early Xenopus pronephros this can't be directly testes. Though pseudotime analysis suggests that both *Xenpous* and mammalian nephrons progress along a similar trajectory to generate nephrons, the comparisons to the developing human kidney indicate similarities between early development and the mature cell types, but that intermediate cell types have differences. Many of the intermediate factors such as *osr1*, *dll1, and lhx1* are present, but likely temporal differences in the gene expression likely leads to different gene expression in intermediate cell types which was can be seen in the scRNA-seq dataset. As an example, *DLL1* in humans is expressed in all three of the nephric lineages. However, its expression is restricted to the proximal tubules at later timepoints. In *Xenopus,* expression of this transcript corresponds with the timing in which the proximal tubules diverge from the distal segments. A similar observation was made for *lef1*. This early divergence is likely a consequence of distinct temporal regulation of gene expression in *Xenopus* and humans required to orchestrate similar developmental programming to generate nephrons.

This study describes the structure and early development of the mesonephric kidney. Given descriptions of this structure are largely anatomical, a more complete spatial and transcriptional makeup of this structure is needed. To obtain a more complete transcriptional profile of the mesonephros scRNA-seq was carried out on the early mesonephric kidney. We find that the *Xenopus* mesonephric kidney is extremely similar to the previously characterized pronephric kidney. *Xenopus* early kidney progenitors are similar to human progenitors with differences in the temporal regulation of gene expression in intermediate cell types, the more developed cells also share similar transcriptional profile. Using the transcriptomic data, the cell types identified were

spatially mapped utilizing a P*pax8::gfp* transgenic as well as *in situ* analysis on markers. Overall, this study uncovers novel insights into the structure and development of the mesonephros.

Acknowledgements

We appreciate the helpful suggestions and advice throughout this project from the members of the laboratories of R. K. Miller, P. D. McCrea, J. Park, as well as M. Kloc. A special thanks to Dr. Yoshihiro Komatsu for the use of equipment in this project. We thank the animal care technicians and veterinarians, including J.C. Whitney and T.H. Gomez who took care of the animals. Also, the NXR for providing cryosperm RRID:SCR_013731. Furthermore, we thank the instructors and teaching assistants of the Cold Spring Harbor Laboratory's Cell & Developmental Biology of Xenopus: Gene Discovery & Disease Course for advanced research training. Thanks to the UTHealth Cancer Genomics Center (CGC) for quick processing of the scRNA-seq samples And to the Soeren S Lienkamp, and Oliver Wessely labs for providing the many plasmids for making in situ probes. Brandy L. Walker M.S. hand drew artwork for figure 6.

Competing Interests

'No competing interests declared'

Funding

National Institute of Diabetes and Digestive and Kidney Diseases, Grant/Award Numbers: R03DK118771 and R01DK115655 to RKM

Author contributions

RKM and SYS initially conceptualized this project. Kidney dissections and single-cell analysis was performed by MEC. Data analysis was performed by MEC with the help of MA, and NL. Writing and figures were initially assembled by MEC. Project administration as well as data and manuscript evaluation were carried out by MEC, RKM and SYS. In situ analysis was carried out by MEC and AR.

Figure Legends

Figure 1: Visualization of mesonephric kidney development and function. A.) Live imaging of P*pax8*::GFP embryos over the stages of mesonephric development. B.) Paraffin embedded section of adult mesonephric kidney tubules stained with acetylated tubulin (green), DAPI (blue) and DIC image. C.) Ventral side of stage 52 embryo along with illustration showing injection of Hoechst and EC-lectin (green) into the heart (brown). D.) Image of the mesonephric kidney after injection of EC-lectin (green) and Hoechst 3342 (blue) into the heart.

Figure 2: Single-cell mRNA sequencing of stage 49-52 mesonephric kidneys. A.) Diagram of kidney isolation on stage 52 *X. laevis,* along with image of kidney before and after isolation. Blue dotted line surrounds both pronephric and mesonephric kidney. Orange dotted line indicates region of kidney isolated. B.) UMAP showing the cell types isolated. C-D.) Analysis of subclustered kidney cells. C.) UMAP of kidney cell types. D) Magnified image of orange box in panel C. E.) Dotplot showing expression of markers in the mesonephros that have been shown to define each segment in the pronephros.

Figure 3: Integration of single-cell data between mesonephric and pronephric kidneys. A.) UMAP showing the integrated dataset. Cluster names as identified by independent analysis, along with separated pronephros and mesonephric samples. Clustering was performed on the joint sample to indicate similar cell types. B.) Dotplot showing normalized expression of kidney gene markers for each segment. Orange dots show expression in the pronephros and blue dots indicate expression in the mesonephros. C.) Dotplot showing genes that have different expression between the pronephros and mesonephros.

Figure 4: Pseudotime analysis of the developing mesonephric kidney. A-B.) Using Monocle 3 pseudotime analysis was performed. Darker blue colors indicate more embryonic lineage, while brighter yellow indicates more differentiated cells. Multiciliated cell were not analyzed indicated in grey. Predicted flow of development based upon Monocle 3 estimates. C.) Subset of embryonic cell types indicated by orange dashed line in D.) Predicted lineage of cell types. F-H) UMAP showing expression of markers of indicated cell types in undeveloped cell types in the early cells.

Figure 5: Comparison between the cell types of the *Xenopus* mesonephric kidney and the adult mouse metanephric kidney. A) Methodology to convert frog data to be compatible with mouse and human datasets. B) UMAP projection showing integrated mouse metanephric and *Xenopus* mesonephric data sets. C) Using the Mouse Kidney Cell Explorer dataset, the top 50 enriched genes for each cluster were identified using the

FindAllMarkers function in Seurat. Using the AddModuleScore function average relative expression for each gene set was calculated for the Xenopus Mesonephric Kidney. Average expression, and percentage of cells that have at least one transcript was displayed for each cluster. Genes with no clear homeolog were ignored.

Figure 6: Spatial analysis of mesonephric cell types. A.) In situ analysis of *six1* kidney progenitor marker B.) Ec-Lectin::FITC and LEL-Lectin::Dylight594 staining of fixed stage 50 embryos. C.) In situ analysis of nephron segments. Stage 52-53 kidneys were stained for indicated probes. Segments each probe labels are indicated by the layout of the *Xenopus* nephron from proximal to distal. Blue numbers above each segment indicate clusters identified by single-cell analysis. Black or white scale bars indicate 1mM. D.) Diagram indicating the model of mesonephric nephron structure.

Citations

1. *Principles of Renal Physiology*, Fifth edn. Springer, 2012.

2. Guder WG, Ross BD. Enzyme distribution along the nephron. *Kidney Int* 1984; **26:** 101-111.

3. Vallon V, Platt KA, Cunard R*, et al.* SGLT2 mediates glucose reabsorption in the early proximal tubule. *J Am Soc Nephrol* 2011; **22:** 104-112.

4. Zaika O, Mamenko M, Berrout J*, et al.* TRPV4 dysfunction promotes renal cystogenesis in autosomal recessive polycystic kidney disease. *J Am Soc Nephrol* 2013; **24:** 604-616.

5. Kramer-Zucker AG, Wiessner S, Jensen AM*, et al.* Organization of the pronephric filtration apparatus in zebrafish requires Nephrin, Podocin and the FERM domain protein Mosaic eyes. *Dev Biol* 2005; **285:** 316-329.

6. Hildebrandt F. Genetic kidney diseases. *Lancet* 2010; **375:** 1287-1295.

7. Hildebrandt F. Decade in review--genetics of kidney diseases: Genetic dissection of kidney disorders. *Nat Rev Nephrol* 2015; **11:** 635-636.

8. Wingert RA, Davidson AJ. The zebrafish pronephros: a model to study nephron segmentation. *Kidney Int* 2008; **73:** 1120-1127.

9. Dressler GR. Advances in early kidney specification, development and patterning. *Development* 2009; **136:** 3863-3874.

10. Vize PD, Jones EA, Pfister R. Development of the Xenopus pronephric system. *Dev Biol* 1995; **171:** 531-540.

11. Ribes D, Fischer E, Calmont A*, et al.* Transcriptional control of epithelial differentiation during kidney development. *J Am Soc Nephrol* 2003; **14 Suppl 1:** S9-15.

12. Zhou X, Vize PD. Proximo-distal specialization of epithelial transport processes within the Xenopus pronephric kidney tubules. *Dev Biol* 2004; **271:** 322-338.

13. Gerlach GF, Wingert RA. Kidney organogenesis in the zebrafish: insights into vertebrate nephrogenesis and regeneration. *Wiley Interdiscip Rev Dev Biol* 2013; **2:** 559-585.

14. Zhou W, Boucher RC, Bollig F*, et al.* Characterization of mesonephric development and regeneration using transgenic zebrafish. *Am J Physiol Renal Physiol* 2010; **299:** F1040-1047.

15. Lametschwandtner A, Minnich B. Renal microvasculature in the adult pipid frog, Xenopus laevis: A scanning electron microscope study of vascular corrosion casts. *J Morphol* 2020; **281:** 725-736.

406 16. Kitagaki J, Ueda Y, Chi X*, et al.* FGF8 is essential for formation of the ductal system in the male reproductive
407 tract. *Development* 2011; **138:** 5369-5378.
408
409 17. Sajithlal G, Zou D, Silvius D*, et al.* Eya 1 acts as a critical regulator for specifying the metanephric mesenchyme.
410 *Dev Biol* 2005; **284:** 323-336.
411
412 18. Rehman S, Ahmed D. Embryology, Kidney, Bladder, and Ureter. *StatPearls*: Treasure Island (FL), 2022.
413
414 19. Diep CQ, Peng Z, Ukah TK*, et al.* Development of the zebrafish mesonephros. *Genesis* 2015; **53:** 257-269.
415
416 20. Fox H. The amphibian pronephros. *Q Rev Biol* 1963; **38:** 1-25.
417
418 21. Krneta-Stankic V, DeLay BD, Miller RK. Xenopus: leaping forward in kidney organogenesis. *Pediatr Nephrol* 2017;
419 **32:** 547-555.
420
421 22. Wingert RA, Davidson AJ. Zebrafish nephrogenesis involves dynamic spatiotemporal expression changes in renal
422 progenitors and essential signals from retinoic acid and irx3b. *Dev Dyn* 2011; **240:** 2011-2027.
423
424 23. Brunskill EW, Aronow BJ, Georgas K*, et al.* Atlas of gene expression in the developing kidney at microanatomic
425 resolution. *Dev Cell* 2008; **15:** 781-791.
426
427 24. Georgas K, Rumballe B, Valerius MT*, et al.* Analysis of early nephron patterning reveals a role for distal RV
428 proliferation in fusion to the ureteric tip via a cap mesenchyme-derived connecting segment. *Dev Biol* 2009; **332:**
429 273-286.
430
431 25. Merchant-Larios R, Villalpando I. Ultrastructural events during early gonadal development in Rana pipiens and
432 Xenopus laevis. *Anat Rec* 1981; **199:** 349-360.
433
434 26. Soofi A, Levitan I, Dressler GR. Two novel EGFP insertion alleles reveal unique aspects of Pax2 function in
435 embryonic and adult kidneys. *Dev Biol* 2012; **365:** 241-250.
436
437 27. Sanchez-Ferras O, Pacis A, Sotiropoulou M*, et al.* A coordinated progression of progenitor cell states initiates
438 urinary tract development. *Nat Commun* 2021; **12:** 2627.
439
440 28. Maulet Y, Lambert RC, Mykita S*, et al.* Expression and targeting to the plasma membrane of xClC-K, a chloride
441 channel specifically expressed in distinct tubule segments of Xenopus laevis kidney. *Biochem J* 1999; **340 (Pt 3):**
442 737-743.
443
444 29. Diep CQ, Mikeasky N, Davidson AJ. *The Zebrafish in Biomedical Research - Chapter 15*. Academic Press: American
445 College of Laboratory Animal Medicine, 2020.
446
447 30. Grimley E, Dressler GR. Are Pax proteins potential therapeutic targets in kidney disease and cancer? *Kidney Int*
448 2018; **94:** 259-267.
449

450 31. Blackburn ATM, Miller RK. Modeling congenital kidney diseases in Xenopus laevis. *Dis Model Mech* 2019; **12**.
451
452 32. Raciti D, Reggiani L, Geffers L*, et al.* Organization of the pronephric kidney revealed by large-scale gene
453 expression mapping. *Genome Biol* 2008; **9:** R84.
454
455 33. Corkins ME, Achieng M, De Lay BD*, et al.* A comparative study of cellular diversity between the Xenopus
456 pronephric and mouse metanephric nephron. *Kidney Int* 2022.
457
458 34. Noble A, Abu-Daya A, Guille M. Cryopreservation of Xenopus Sperm and In Vitro Fertilization Using Frozen
459 Sperm Samples. *Cold Spring Harb Protoc* 2022; **2022**.
460
461 35. Pearl EJ, Grainger RM, Guille M*, et al.* Development of Xenopus resource centers: the National Xenopus
462 Resource and the European Xenopus Resource Center. *Genesis* 2012; **50:** 155-163.
463
464 36. Butler K, Zorn AM, Gurdon JB. Nonradioactive in situ hybridization to xenopus tissue sections. *Methods* 2001; **23:**
465 303-312.
466
467 37. Willsey HR. Whole-Mount RNA In Situ Hybridization and Immunofluorescence of Xenopus Embryos and
468 Tadpoles. *Cold Spring Harb Protoc* 2021; **2021:** pdb prot105635.
469
470 38. Butler A, Hoffman P, Smibert P*, et al.* Integrating single-cell transcriptomic data across different conditions,
471 technologies, and species. *Nat Biotechnol* 2018; **36:** 411-420.
472
473 39. Hao Y, Hao S, Andersen-Nissen E*, et al.* Integrated analysis of multimodal single-cell data. *Cell* 2021; **184:** 3573-
474 3587 e3529.
475
476 40. Ochi H, Tamai T, Nagano H*, et al.* Evolution of a tissue-specific silencer underlies divergence in the expression of
477 pax2 and pax8 paralogues. *Nat Commun* 2012; **3:** 848.
478
479 41. Buisson I, Le Bouffant R, Futel M*, et al.* Pax8 and Pax2 are specifically required at different steps of Xenopus
480 pronephros development. *Dev Biol* 2015; **397:** 175-190.
481
482 42. Kaku Y, Taguchi A, Tanigawa S*, et al.* PAX2 is dispensable for in vitro nephron formation from human induced
483 pluripotent stem cells. *Sci Rep* 2017; **7:** 4554.
484
485 43. Traykova-Brauch M, Schonig K, Greiner O*, et al.* An efficient and versatile system for acute and chronic
486 modulation of renal tubular function in transgenic mice. *Nat Med* 2008; **14:** 979-984.
487
488 44. Corkins ME, Hanania HL, Krneta-Stankic V*, et al.* Transgenic Xenopus laevis Line for In Vivo Labeling of Nephrons
489 within the Kidney. *Genes (Basel)* 2018; **9**.
490
491 45. Tran U, Pickney LM, Ozpolat BD*, et al.* Xenopus Bicaudal-C is required for the differentiation of the amphibian
492 pronephros. *Dev Biol* 2007; **307:** 152-164.
493

494 46. Self M, Lagutin OV, Bowling B*, et al.* Six2 is required for suppression of nephrogenesis and progenitor renewal in
495 the developing kidney. *EMBO J* 2006; **25:** 5214-5228.

496
497 47. Combes AN, Zappia L, Er PX*, et al.* Single-cell analysis reveals congruence between kidney organoids and human
498 fetal kidney. *Genome Med* 2019; **11:** 3.

499
500 48. DeLay BD, Corkins ME, Hanania HL*, et al.* Tissue-Specific Gene Inactivation in Xenopus laevis: Knockout of lhx1 in
501 the Kidney with CRISPR/Cas9. *Genetics* 2018; **208:** 673-686.

502
503 49. Cirio MC, Hui Z, Haldin CE*, et al.* Lhx1 is required for specification of the renal progenitor cell field. *PLoS One*
504 2011; **6:** e18858.

505
506 50. Tirosh I, Izar B, Prakadan SM*, et al.* Dissecting the multicellular ecosystem of metastatic melanoma by single-cell
507 RNA-seq. *Science* 2016; **352:** 189-196.

508
509 51. Trapnell C, Cacchiarelli D, Grimsby J*, et al.* The dynamics and regulators of cell fate decisions are revealed by
510 pseudotemporal ordering of single cells. *Nat Biotechnol* 2014; **32:** 381-386.

511
512 52. O'Brien LL, Guo Q, Lee Y*, et al.* Differential regulation of mouse and human nephron progenitors by the Six
513 family of transcriptional regulators. *Development* 2016; **143:** 595-608.

514
515 53. Getwan M, Lienkamp SS. Toolbox in a tadpole: Xenopus for kidney research. *Cell Tissue Res* 2017; **369:** 143-157.

516
517 54. Li L, Wen L, Gong Y*, et al.* Xenopus as a model system for the study of GOLPH2/GP73 function: Xenopus GOLPH2
518 is required for pronephros development. *PLoS One* 2012; **7:** e38939.

519
520 55. Miller RK, Canny SG, Jang CW*, et al.* Pronephric tubulogenesis requires Daam1-mediated planar cell polarity
521 signaling. *J Am Soc Nephrol* 2011; **22:** 1654-1664.

522
523 56. Gerth VE, Zhou X, Vize PD. Nephrin expression and three-dimensional morphogenesis of the Xenopus pronephric
524 glomus. *Dev Dyn* 2005; **233:** 1131-1139.

525
526 57. Alarcon P, Rodriguez-Seguel E, Fernandez-Gonzalez A*, et al.* A dual requirement for Iroquois genes during
527 Xenopus kidney development. *Development* 2008; **135:** 3197-3207.

528
529 58. Mead PE, Parganas E, Ohtsuka S*, et al.* Evi-1 expression in Xenopus. *Gene Expr Patterns* 2005; **5:** 601-608.

530
531 59. DeLay BD, Baldwin TA, Miller RK. Dynamin Binding Protein Is Required for Xenopus laevis Kidney Development.
532 *Front Physiol* 2019; **10:** 143.

533
534 60. Vize PD. The chloride conductance channel ClC-K is a specific marker for the Xenopus pronephric distal tubule
535 and duct. *Gene Expr Patterns* 2003; **3:** 347-350.

536

537 61. Quigley IK, Stubbs JL, Kintner C. Specification of ion transport cells in the Xenopus larval skin. *Development* 2011;
538 **138:** 705-714.

539

540 62. Vize PD. *The Kidney - Chapter 1* Elsevier Inc., 2002.

541

542 63. Bertram JF, Douglas-Denton RN, Diouf B*, et al.* Human nephron number: implications for health and disease.
543 *Pediatr Nephrol* 2011; **26:** 1529-1533.

544

545 64. Villalpando I, Merchant-Larios H. Determination of the sensitive stages for gonadal sex-reversal in Xenopus
546 laevis tadpoles. *Int J Dev Biol* 1990; **34:** 281-285.

547

548 65. Kalt MR. Ultrastructural observations on the germ line of Xenopus laevis. *Z Zellforsch Mikrosk Anat* 1973; **138:**
549 41-62.

550

551 66. Mawaribuchi S, Takahashi S, Wada M*, et al.* Sex chromosome differentiation and the W- and Z-specific loci in
552 Xenopus laevis. *Dev Biol* 2017; **426:** 393-400.

553

554 67. Demirci FY, Chang MH, Mah TS*, et al.* Proximal renal tubular acidosis and ocular pathology: a novel missense
555 mutation in the gene (SLC4A4) for sodium bicarbonate cotransporter protein (NBCe1). *Mol Vis* 2006; **12:** 324-
556 330.

557

558

559

Figure 1

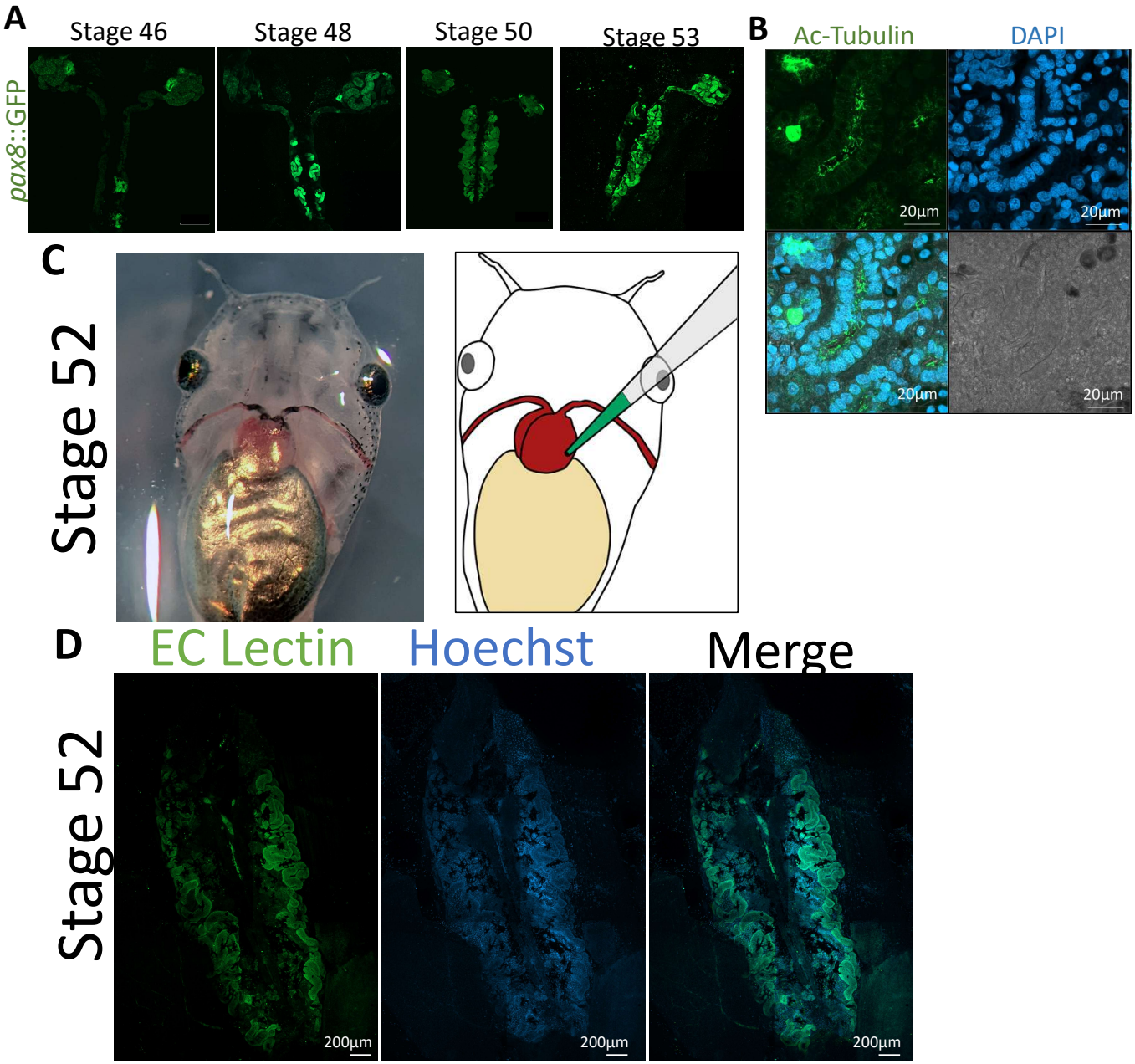
A
Stage 46
Stage 48
Stage 50
Stage 53
pax8::GFP
B
Ac-Tubulin
DAPI
20µm
20µm
20µm
20µm
C
Stage 52
D
EC Lectin
Hoechst
Merge
Stage 52
200µm
200µm
200µm

Figure 2

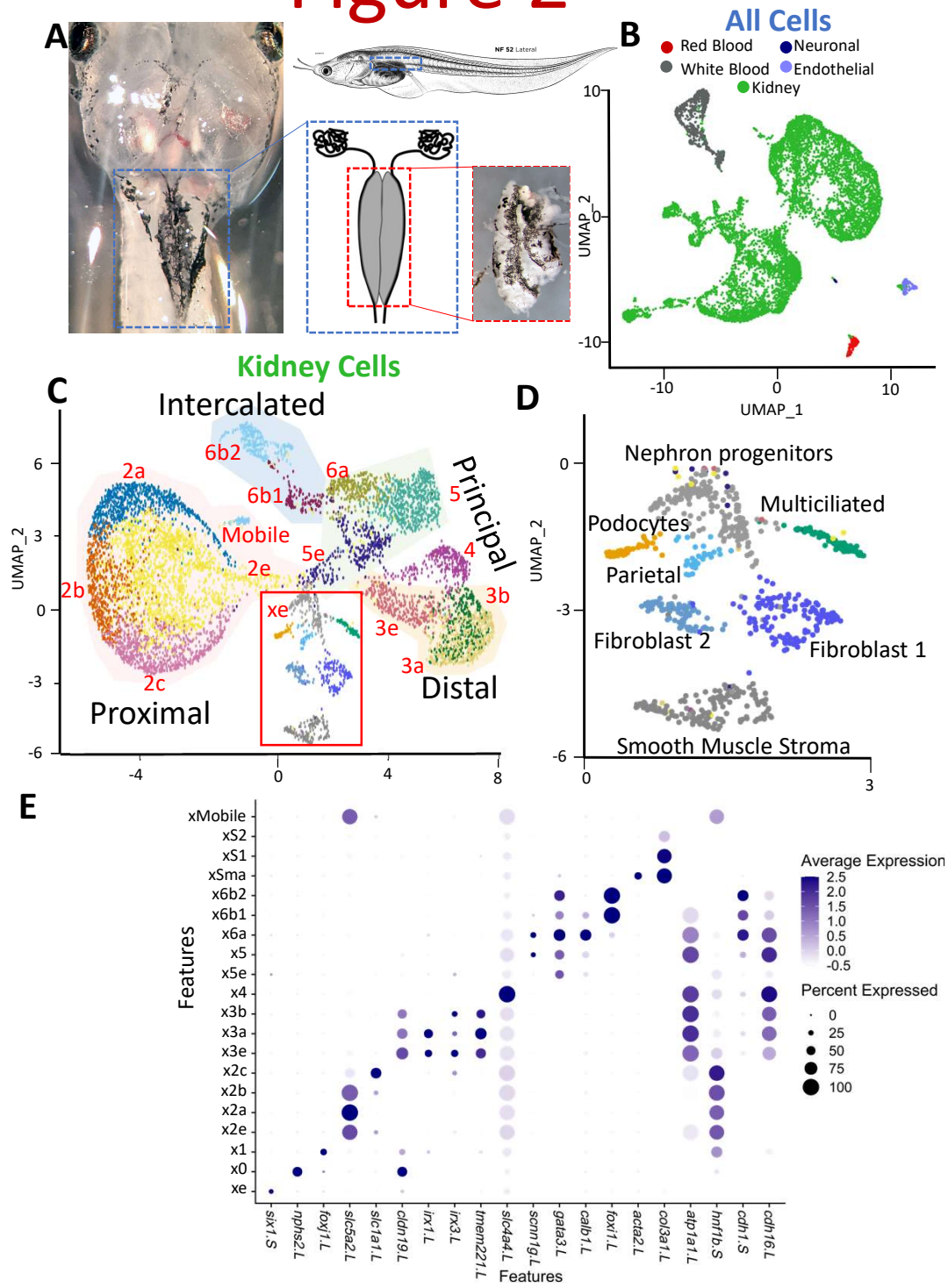
A
NF 52 Lateral
B
All Cells
Red Blood
Neuronal
White Blood
Endothelial
Kidney
UMAP_2
UMAP_1
Kidney Cells
C
Intercalated
Principal
Proximal
Distal
Mobile
2a
2b
2c
2e
6b2
6b1
6a
5
5e
4
3b
3e
3a
xe
UMAP_2
D
Nephron progenitors
Multiciliated
Podocytes
Parietal
Fibroblast 2
Fibroblast 1
Smooth Muscle Stroma
UMAP_2
E
Features
xMobile
xS2
xS1
xSma
x6b2
x6b1
x6a
x5
x5e
x4
x3b
x3a
x3e
x2c
x2b
x2a
x2e
x1
x0
xe
six1.S
nphs2.L
foxj1.L
slc5a2.L
slc1a1.L
cldn19.L
irx1.L
irx3.L
tmem221.L
slc4a4.L
scnn1g.L
gata3.L
calb1.L
foxi1.L
acta2.L
col3a1.L
atp1a1.L
hnf1b.S
cdh1.S
cdh16.L
Features
Average Expression
2.5
2.0
1.5
1.0
0.5
0.0
-0.5
Percent Expressed
0
25
50
75
100

Figure 3

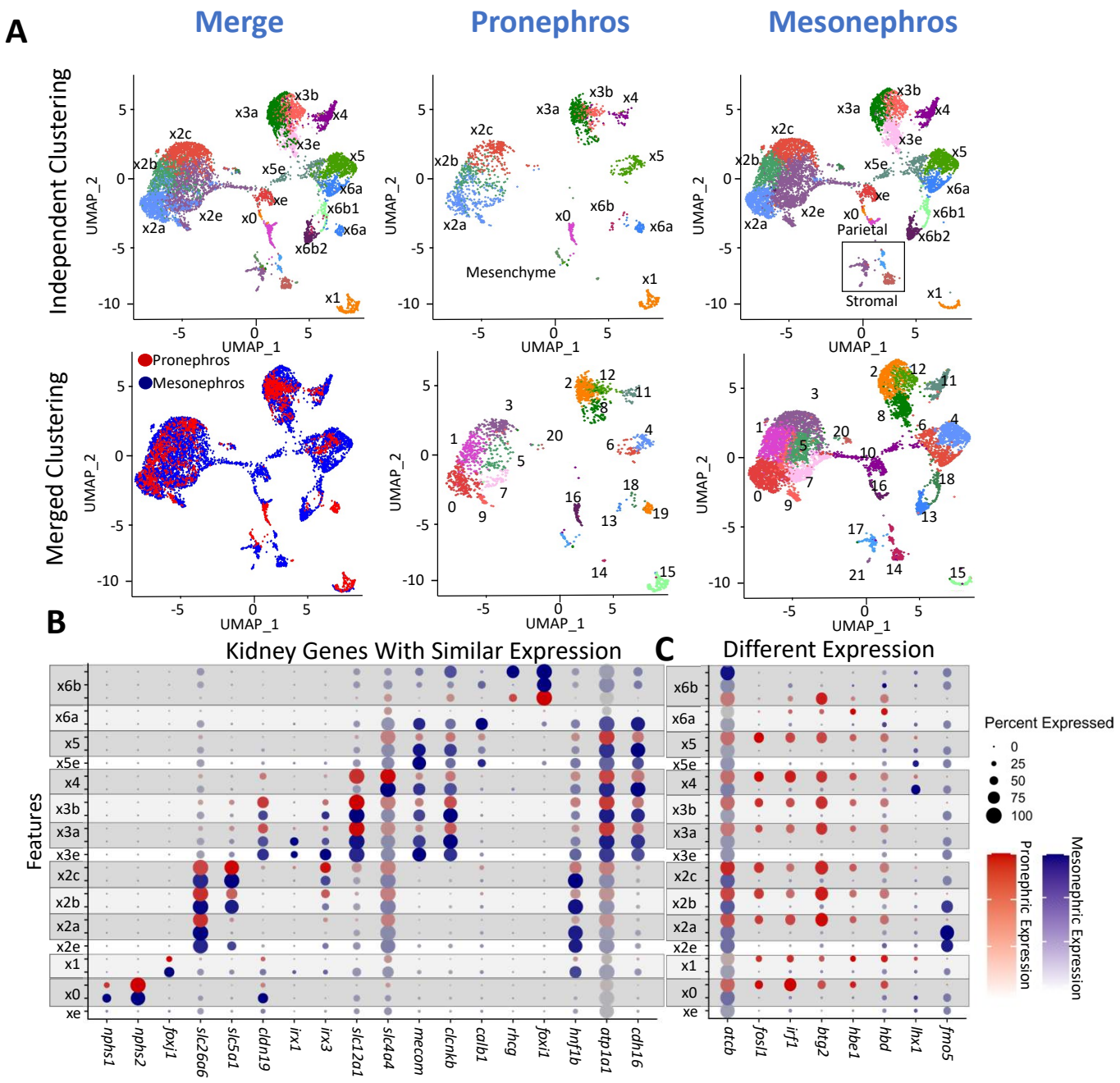
A
Merge
Pronephros
Mesonephros
Independent Clustering
Merged Clustering
UMAP_1
UMAP_2
Pronephros
Mesonephros
Mesenchyme
Parietal
Stromal
B
Kidney Genes With Similar Expression
C
Different Expression
Features
nphs1
nphs2
foxi1
slc26a6
slc5a1
cldn19
irx1
irx3
slc12a1
slc4a4
mecom
clcnkb
calb1
rhcg
foxi1
hnf1b
atp1a1
cdh16
atcb
fosl1
irf1
btg2
hbe1
hbd
lhx1
fmo5
Percent Expressed
0
25
50
75
100
Pronephric Expression
Mesonephric Expression

Figure 4

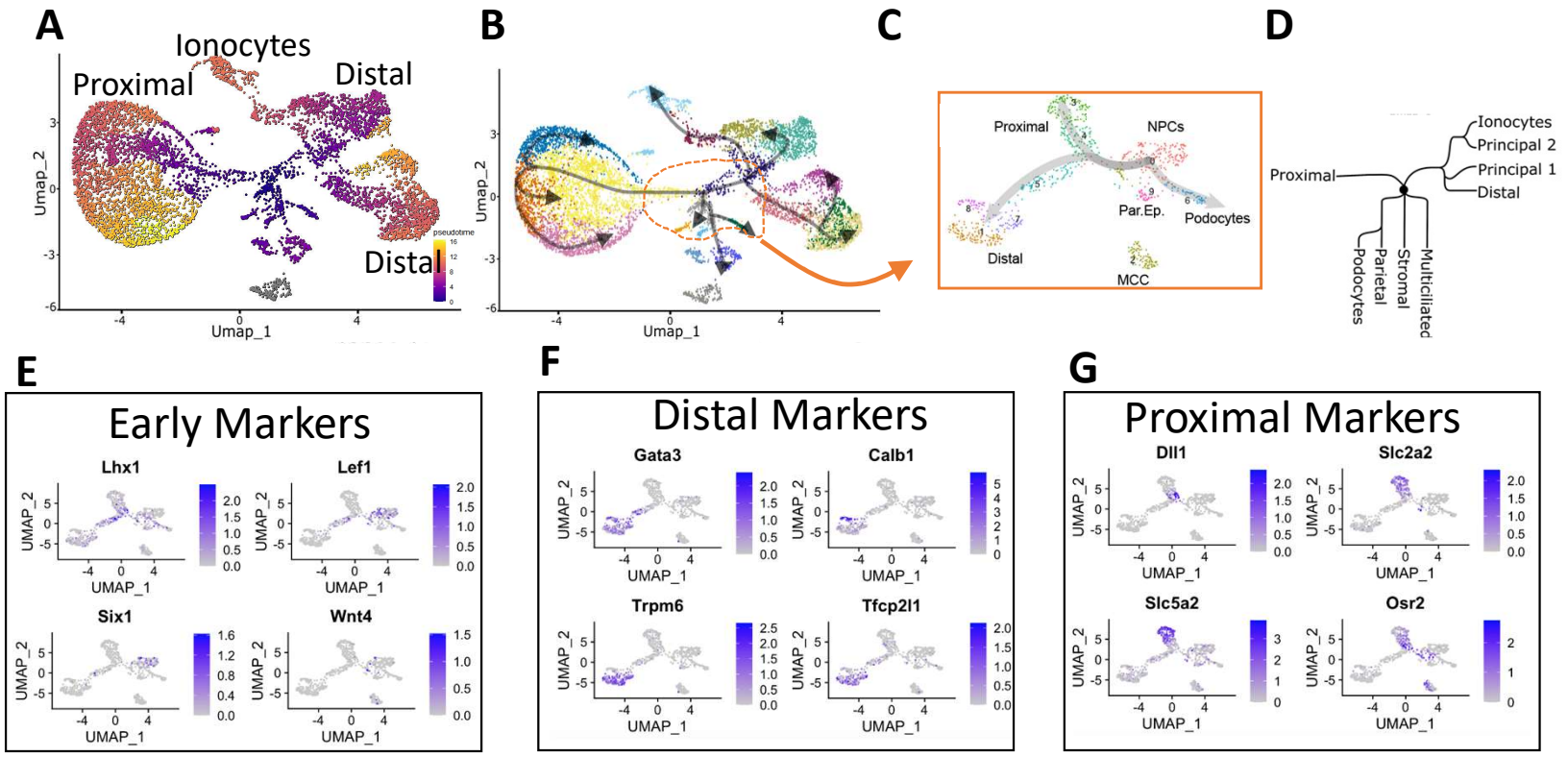
A
Ionocytes
Proximal
Distal
Distal
Umap_2
Umap_1
pseudotime
B
Umap_2
Umap_1
C
Proximal
NPCs
Par.Ep.
Podocytes
Distal
MCC
D
Ionocytes
Principal 2
Principal 1
Distal
Proximal
Podocytes
Parietal
Stromal
Multiciliated
E
Early Markers
Lhx1
Lef1
Six1
Wnt4
UMAP_2
UMAP_1
F
Distal Markers
Gata3
Calb1
Trpm6
Tfcp2l1
UMAP_2
UMAP_1
G
Proximal Markers
Dll1
Slc2a2
Slc5a2
Osr2
UMAP_2
UMAP_1

Figure 5

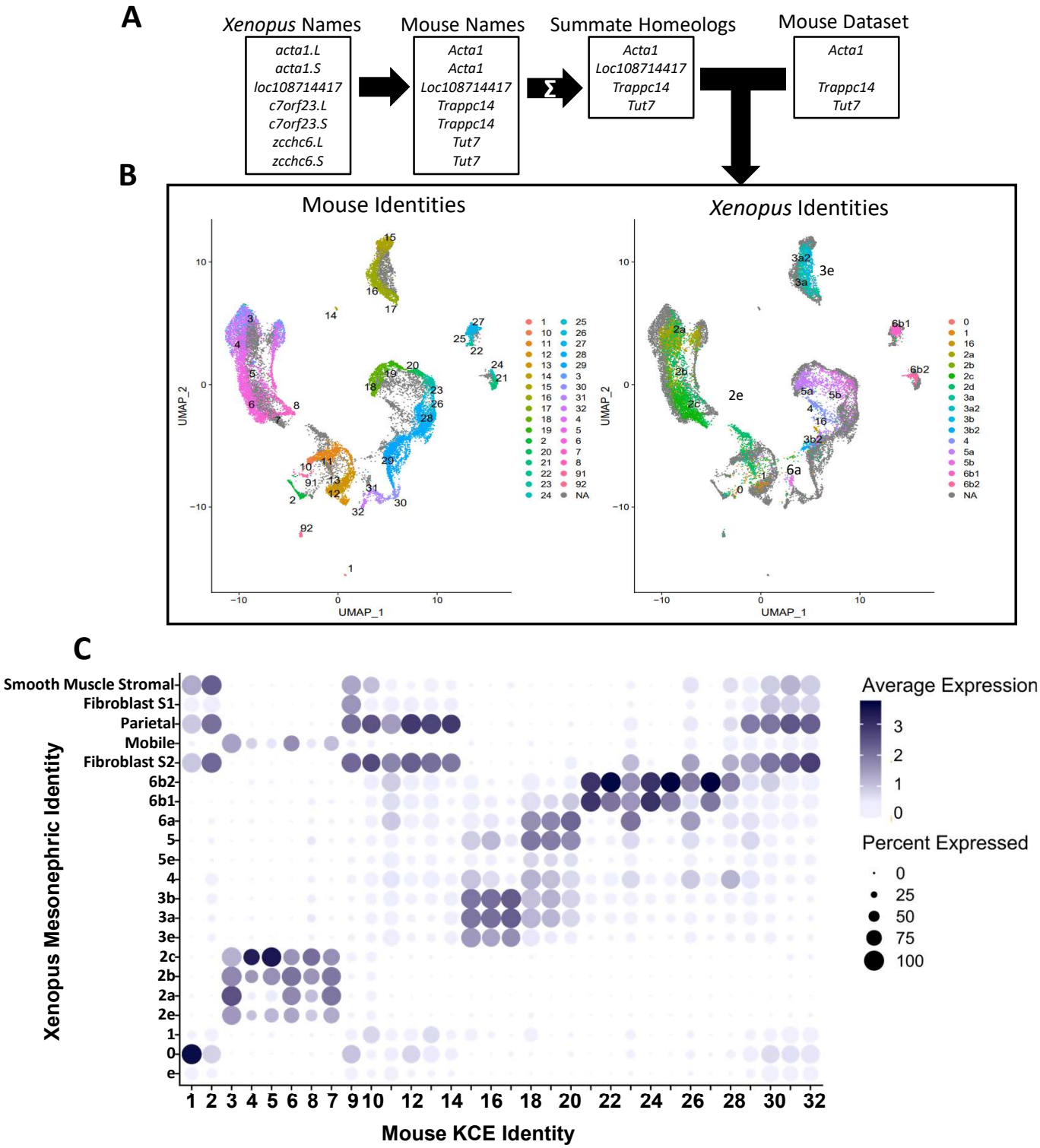

Figure 5 – Comparison between the cell types of the *Xenopus* mesonephric kidney and the adult mouse metanephric kidney. **A)** Methodology to convert frog data to be compatible with mouse and human datasets. **B)** UMAP projection showing integrated mouse metanephric and *Xenopus* mesonephric data sets. **C)** Using the Mouse Kidney Cell Explorer dataset [1], the top 50 enriched genes for each cluster was identified using the FindAllMarkers function in Seurat. Using the AddModuleScore [2] function average relative expression for each gene set was calculated for the Xenopus Mesonephric Kidney. Average expression, and percentage of cells that have at least one transcript was displayed for each cluster. Genes with no clear homeolog were ignored.

1. Ransick A, Lindstrom NO, Liu J, et al. Single-Cell Profiling Reveals Sex, Lineage, and Regional Diversity in the Mouse Kidney. Dev Cell 2019; 51: 399-413 e397.
2. Tirosh I, Izar B, Prakadan SM, et al. Dissecting the multicellular ecosystem of metastatic melanoma by single-cell RNA-seq. Science 2016; 352: 189-196.

Figure 6

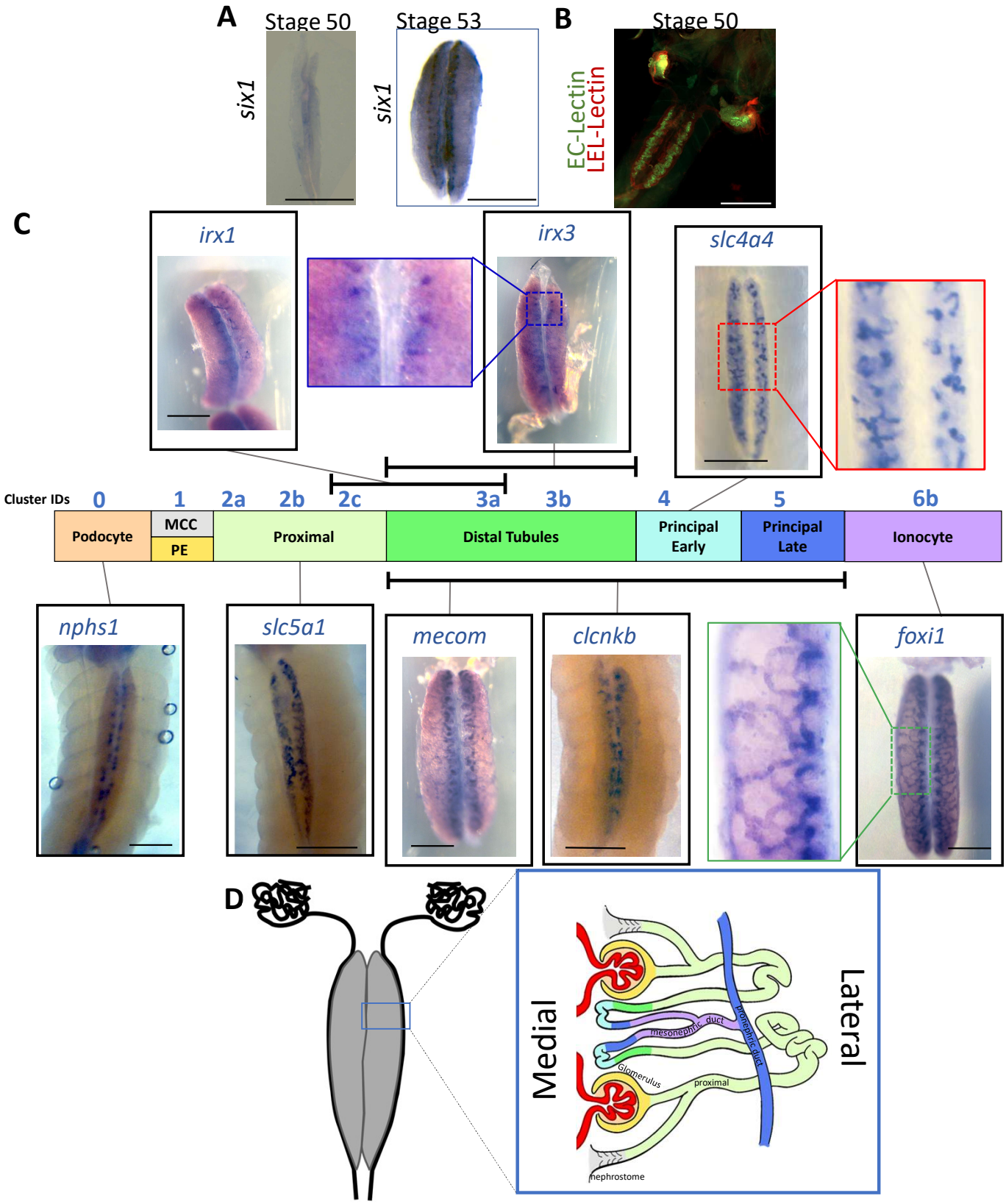
A
Stage 50
Stage 53
six1
six1
B
Stage 50
EC-Lectin
LEL-Lectin
C
irx1
irx3
slc4a4
Cluster IDs
0
1
2a
2b
2c
3a
3b
4
5
6b
Podocyte
MCC
PE
Proximal
Distal Tubules
Principal Early
Principal Late
Ionocyte
nphs1
slc5a1
mecom
clcnkb
foxi1
D
Medial
Lateral
mesonephric duct
paranephric duct
Glomerulus
proximal
nephrostome

Supplemental Figure 1

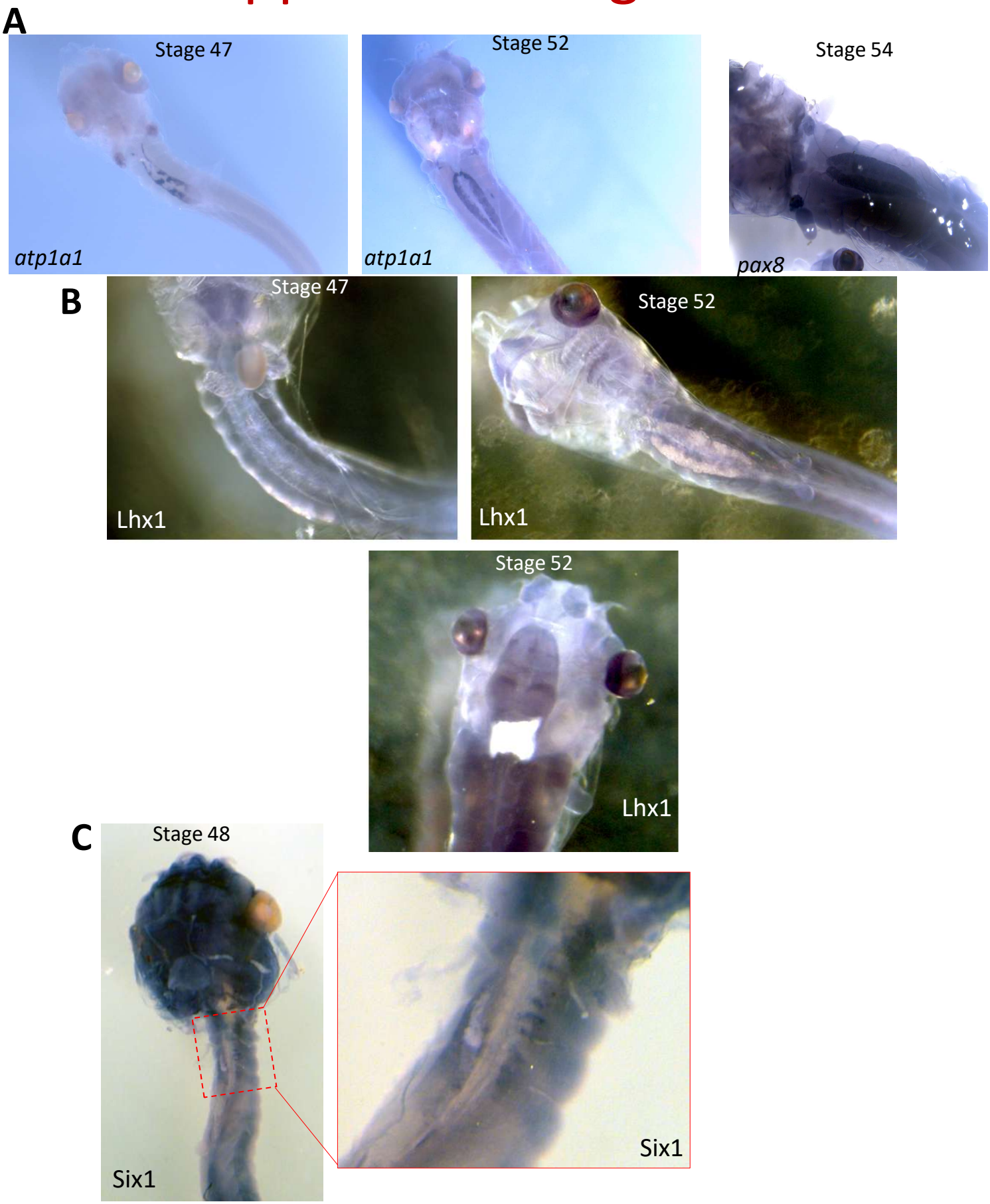

Figure S1: A.) Insitu analysis of kidney nephron markers atp1a1, pax8. B.) *lhx1* in situ of stage 47 and 52 kidney and brain staining. C.) Staining of the kidney progenitor marker *six1*.

Supplemental Figure 2

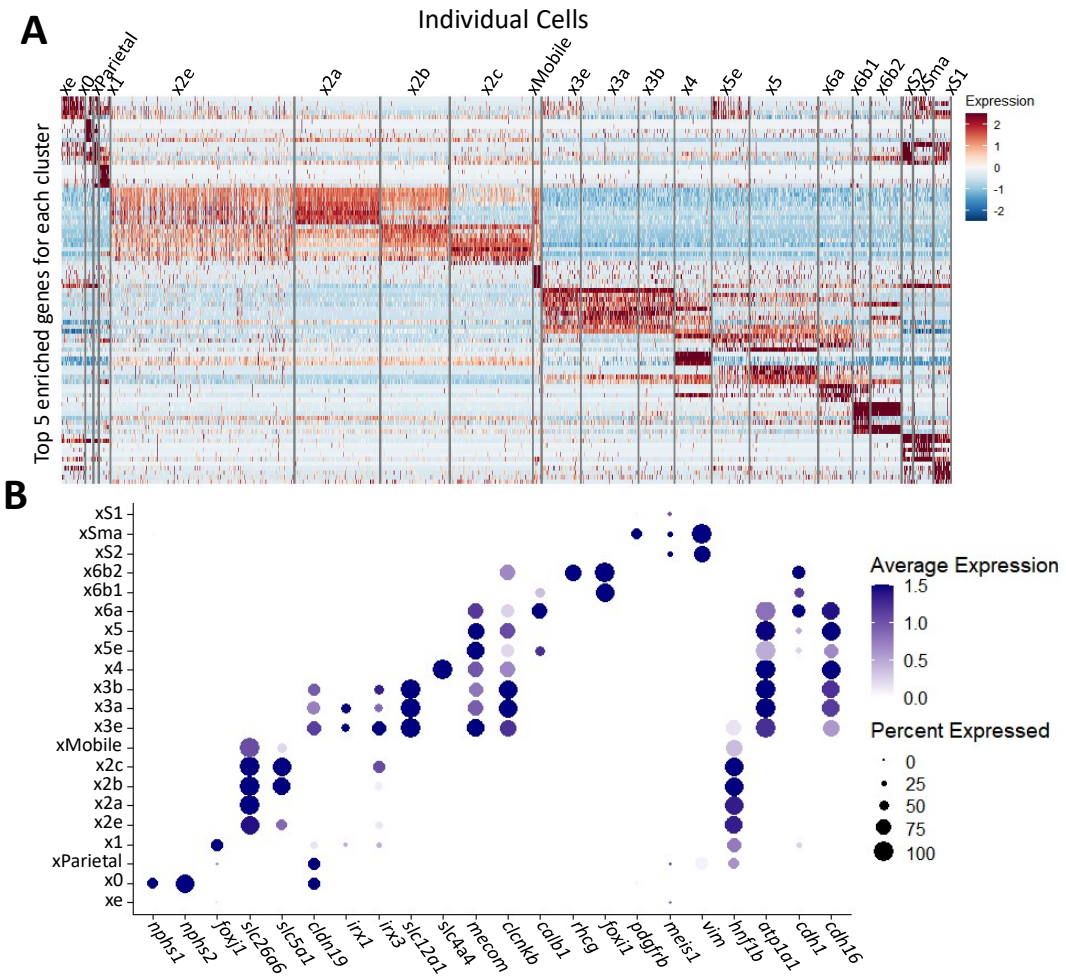

Figure S2: A.) Heatmap showing the top 10 genes for each cluster after combining homeologs. Each row indicates expression of an individual gene while each column indicates a single cell. Dotplot showing expression of kidney segment genes.

Figure Supp 3

Non-Kidney Cell Types

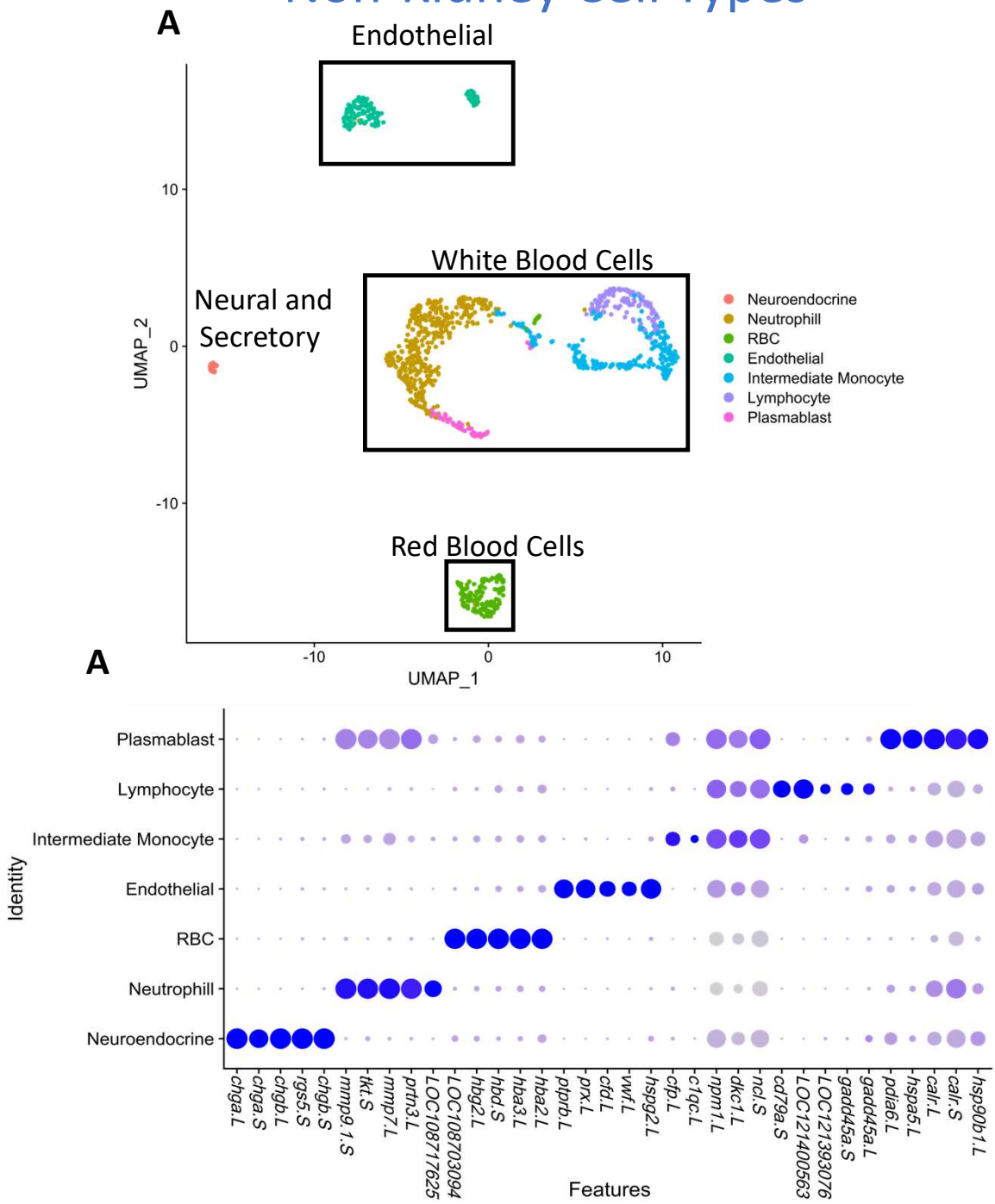

Figure S4 – Non-kidny cells were isolated and identified. **A)** UMAP projection of non-kidney cells. **B)** Dotplot showing top 5 enriched genes for each cell types.